Structural Engineering and Mechanics, Vol. 17, No. 5 (2004) 691-706
DOI: http://dx.doi.org/10.12989/sem.2004.17.5.691

Evaluation of shear lag parameters for beam-to-column connections in steel piers

Won-Sup Hwang† and Young-Pil Kim‡

Department of Civil Engineering, Inha University, 253 Younghyun-Dong, Nam-Gu, Incheon 402-751, Korea

Yong-Myung Park‡†

Department of Civil Engineering, Pusan National University, 30 Jangjeon-Dong, Geumjeong-Gu, Pusan 609-735, Korea

(Receive July 21, 2003, Accepted November 27, 2003)

Abstract. The paper presents shear lag parameters for beam-to-column connections in steel box piers. Previous researches have analyzed beam-to-column connections in steel piers using a shear lag parameter η_o obtained from a simple beam model, which is not based on a reasonable design assumption. Instead, the current paper proposes a cantilever beam model and has proved the effectiveness through theoretical and experimental studies. The paper examines the inaccuracy of the previous researches by estimating the effective width, the width-span length ratio L/b, and the sectional area ratio S of a cantilever beam. Two different shear lag parameters are defined using the cantilever model and the results are compared each other. The first type of shear lag parameter η_c of a cantilever beam is derived using additional moments from various stress distribution functions while the other shear lag parameter η_{eff} of a cantilever beam is defined based on the concept of the effective width. An evaluation method for shear lag stresses has been investigated by comparing analytical stresses with test results. Through the study, it could be observed that the shear lag parameter η_{eff} agrees with η_c obtained from the 2^{nd} order stress distribution function. Also, it could be observed that the shear lag parameter η_c using the 4^{th} order stress distribution function almost converges to the upper bound of test results.

Key words: beam-to-column connection; shear lag parameter; additional moment; stress distribution function; effective width.

1. Introduction

Recently, steel piers have been widely applied for pier structures of urban overpasses and elevated structures in East Asian countries due to the small space requirements, excellent earthquake resistance capacity, and less construction term. However, at the T-type or framed beam-to-column connections of box-sectioned steel piers as illustrated in Fig. 1, it has been widely acknowledged

† Associate Professor
‡ Ph.D. Candidate
‡† Assistant Professor

that serious shear lag and also stress concentrations may occur due to abrupt direction changes in member forces. Therefore, it has been highly required to handle these problems properly in the design stage.

In the early study on welded steel connections, Beedle *et al*. (1951) proposed a stress and strength evaluation method for a H-sectioned beam-to-column connection by assuming that stresses are uniform in flanges and webs. Fielding and Huang (1971) indicated that the strength of beam-to-column connection of a H-sectioned frame is reduced due to the axial force in column. However, they could not notice shear lag phenomenon at the flange of connection.

By recognizing shear lag phenomenon at box-sectioned beam-to-column connections of pier structure, Okumura and Ishizawa (1968) carried out theoretical and experimental studies using a simple beam model subjected to a concentrated mid-span load and suggested an evaluation method for shear lag stresses as a result. However, they overlooked a problem in assuming internal forces at the welded connection where the distribution of bending moments is closer to that of a cantilever beam rather than that of a simple beam. In addition, Okumura and Ishizawa (1968) did not consider the effective width of the flange plate seriously in estimating the shear lag and stress concentration at the connection. Instead of using a simple beam model, Nakai *et al*. (1992) suggested an equation for the shear lag stress from a study using an overhanged beam model with additional moments due to shear deformation occurred at the connection. However, the result of Nakai *et al*. was also not much different from that of Okumura and Ishizawa because they also did not take reasonable account of the similarity between the internal forces of a beam-to-column connection and the moment distribution of a cantilever beam.

Shear lag in box girders was firstly studied by Reisser (1946), and evaluation of shear lag stress had been studied by many investigators. Malcolm and Redwood (1970) suggested analytical procedure using stiffener-sheet solution. Kuzmanović and Graham (1981) found the minimum potential energy principle was a suitable approach to evaluate the shear lag in box girders. Chang and Zheng (1987) analyzed shear lag effects in cantilever box girders through a variational approach on the additional moment using different analytical procedures under various types of loadings. Recently, the substructuring analysis method for shear lag stress using the conditions of compatibility and equilibrium was introduced by Fafitis and Rong (1996), and Lee and Wu (2000)

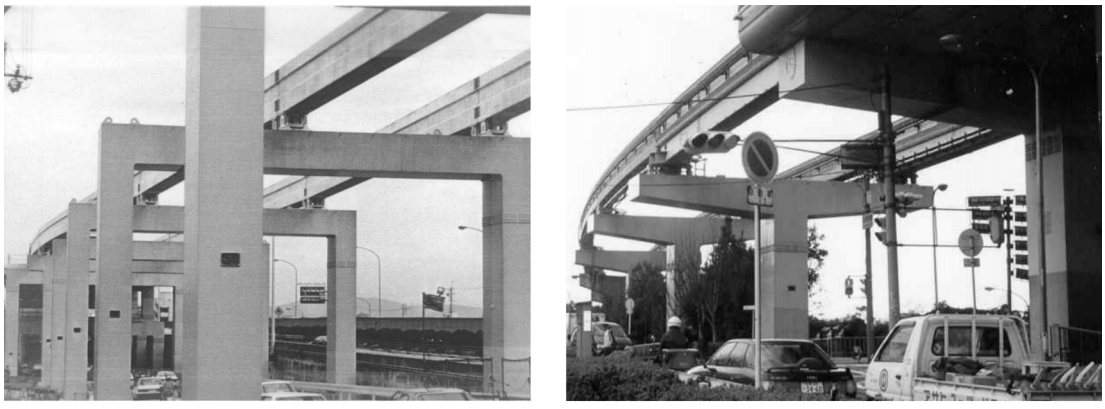

(a) Frame type pier (b) T type pier

Fig. 1 Beam-to-column connections of steel box piers

improved the inefficiency of traditional finite element analysis using uniform meshes in the solution of shear lag stress. Wang (1997) derived an energy equation for the lateral buckling of thin-walled members with openings considering shear lag phenomenon. Also, Luo *et al.* (2002) carried out experimental study on the shear lag effect of box girder with varying depth. However, these studies have been recognized that the complicated equations by many investigators are not so practical for the design of box girders and box-sectioned connections. Also, their studies have been limited to box girders only and did not considered that the shear lag stress of the box-sectioned beam-to-column connection is much higher than that of box girders.

Therefore, the current paper simplifies the equations based on Chang and Zheng and develops an adequate design methodology for the pier connection behavior with shear lag phenomenon. Especially, additional moment of a cantilever beam under concentrated load, which is a new and more reasonable concept to evaluate the shear lag stress of connection, is introduced and applied to a typical box-sectioned connection. Also, the effective width ratio b_e/b using the cantilever model is estimated and the influences of two variables of the width to span length ratio L/b and sectional area ratio $S(=A_w/A_f)$ on the shear lag stress have been investigated. Shear lag parameters depending on the variables of L/b, S, and effective widths are formulated and their adequacy has been examined by comparing analytical outcomes with experimental results.

2. Review of the previous studies

As shown in Fig. 2, the normal stress $\sigma_x(y)$ at the flange of a box section distributes uniformly with σ_b along the y-axis based on the elementary beam theory. However, at the intersection of the flange and web where $y = \pm b'$, the actual maximum normal stress $\sigma_{x,\max}(y = \pm b')$ is higher than the average normal stress of σ_b. This high stress due to the transfer of the shear force from the web to the flange edge is called the shear lag phenomenon (Timoshenko and Goodier 1987).

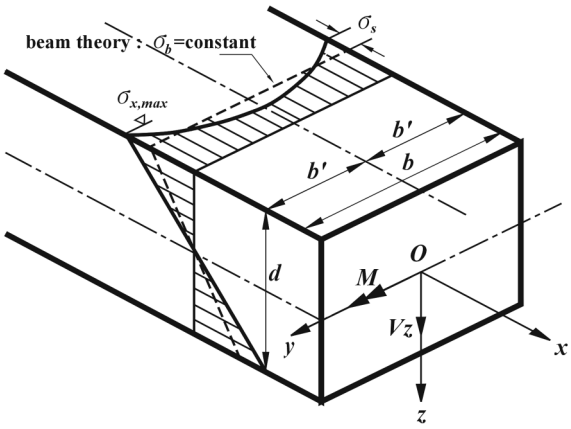

Fig. 2 Normal stress distribution of box beam

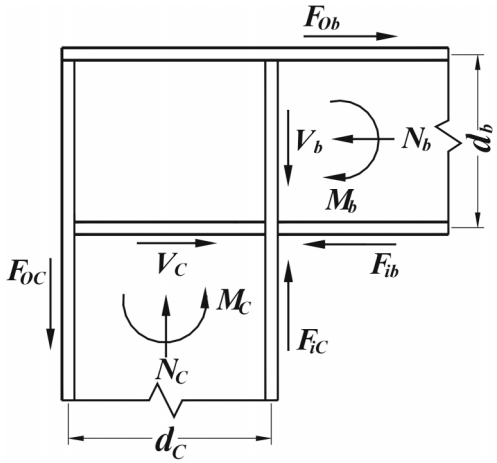

Fig. 3 Internal forces acting on a connection

In the box-sectioned beam-to-column connection, the bending moments in the beam and column are transformed into the concentrated forces in flanges by assuming that the flanges almost resist the moments (Beedle *et al.* 1951, Okumura and Ishizawa 1968). Therefore, the internal concentrated forces F_{ib} and F_{ic}, acting on the flanges of a box-sectioned column and beam at the connection, as depicted in Fig. 3, are defined as follows.

$$F_{ib} = \frac{M_b}{d_b} + \frac{N_b}{2}, \qquad F_{ic} = \frac{M_c}{d_c} + \frac{N_c}{2} \tag{1}$$

where M_b, M_c = moment, N_b, N_c = axial force, d_b, d_c = depth of beam and column sections, respectively. These internal forces F_{ib} and F_{ic} act as shear forces to the column and beam and thus the shear lag phenomenon may occur.

To evaluate the maximum normal stress at the flange, it is required to compute shear lag stress σ_s in Fig. 2 as well as the average vertical stress σ_b from bending moments and axial forces. Okumura and Ishizawa (1968) suggested Eq. (2a) for the shear lag stress σ_s by introducing a shear lag parameter η_o from a simple beam model under a concentrated mid-span load P as shown in Fig. 4.

$$\sigma_s = \eta_o \cdot \left(\frac{b}{d}\frac{F_i}{A_w}\right) \tag{2a}$$

where b, d = width and depth of the beam, F_i = internal concentrated force of the flange, A_w = area of the web, η_o = shear lag parameter by Okumura defined by Eq. (2b), respectively.

$$\eta_o = \sum_{n=1}^{\infty} \frac{6}{\pi^2}\frac{L}{b'}\left(\frac{3}{S+3}\right)\left(\frac{S(1-b_e'/b')}{S+3(b_e'/b')}\right)\frac{1}{n^2} \tag{2b}$$

in which b' = half width of beam, S = sectional area ratio($=A_w/A_f$), b_e' = effective half width of beam, and $\frac{b_e'}{b'} = \frac{\cosh\zeta b' \sinh\zeta b' + \zeta b'}{2\zeta b' \cosh^2 \zeta b'}$ = effective width ratio with $\zeta b' = n\pi\frac{b'}{L}$, respectively.

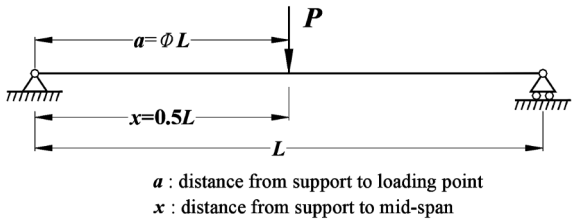

Fig. 4 Simple beam model with span length L

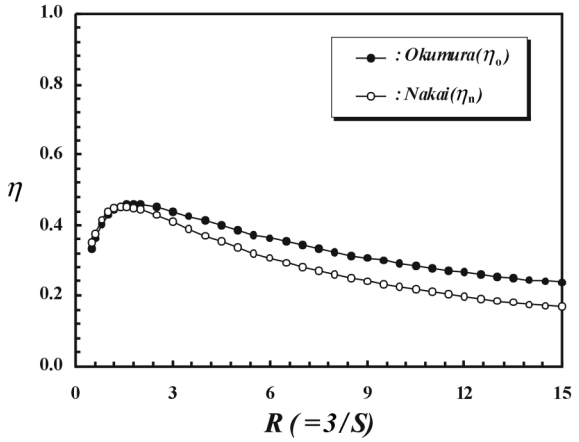

Fig. 5 Comparison of shear lag parameters

However, the use of a simple beam conflicts with the actual observation that the bending moment distribution at a connection is closer to that of a cantilever beam. In addition, since the shear lag parameter η_o of Okmura and Ishizawa is expressed by power series, an additional diagram of Fig. 5 is required for practical applications. With a recognition of this problem, Nakai *et al*. (1992) used an overhanged beam model and suggested a shear lag parameter η_n of Eq. (3) considering an additional moment due to shear deformation.

$$\eta_n = 3.273\frac{R}{(R+1)\sqrt{(R+1)(R+6)}} \tag{3}$$

where R = sectional area ratio(= $3A_f/A_w = 3/S$)

Shear lag parameters for the two cases are compared in Fig. 5. From the figure, it can be observed that the difference is almost negligible although the two parameters of η_o and η_n deviate a little bit as $R > 2.0$.

3. Effective width of a box section

3.1 Effective width of a simple beam

At the mid-span of a box-sectioned simple beam subjected to a concentrated load P as shown in Fig. 4, the normal stress distribution is illustrated in Fig. 7. The effective width ratio ($b_e/b = 2b_e'/2b'$) at the mid-span is given by Eq. (4a) (Komatsu 1974).

$$\frac{b_e}{b} = 1 - \frac{\sqrt{1.5\omega/(1.2-\kappa)\lambda}}{3\phi(1-\phi)(L/b') + \kappa\sqrt{1.5\omega/(1.2-\kappa)\lambda}} \tag{4a}$$

where ν = Poisson's ratio of steel (= 0.3), ϕ = coefficient for distance from support to the point under consideration, $\omega = \frac{1}{1-\nu}$, $\kappa = \frac{A_{fc}}{A} + \frac{I_{fc}}{I} = \frac{2S+3}{(S+3)(S+1)}$, A and A_{fc} are the area of the box section and the compression flange, respectively. I and I_{fc} are the area moment of inertia of the box section and the compression flange, respectively. The constant λ in Eq. (4b) is defined as.

$$\begin{aligned} \lambda &= 1.0 \qquad \text{for} \quad L/b' \geq 5.0 \\ &= \tanh\left(\frac{L/b}{2\omega}\frac{\sqrt{1.5\omega}}{1.2-\kappa}\right) \qquad \text{for} \quad L/b' < 5.0 \end{aligned} \tag{4b}$$

At the mid-span of a simple beam where $\phi = 0.5$, Eq. (4a) reduces to Eq. (5) and could be expressed in terms of L/b' and S.

$$\frac{b_e}{b} = 1 - \frac{4.63\sqrt{\frac{(S+3)(S+1)}{12S^2+28S+6}}}{0.75\frac{L}{b'} + \frac{2S+3}{(S+3)(S+1)}\left(4.63\sqrt{\frac{(S+3)(S+1)}{12S^2+28S+6}}\right)} \tag{5}$$

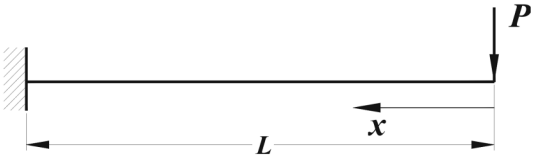

Fig. 6 Cantilever beam model

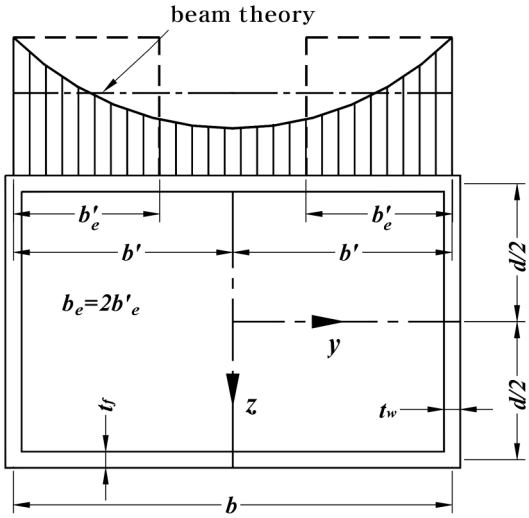

Fig. 7 Effective width of box section

3.2 Effective width of a cantilever beam

3.2.1 The 2nd order stress distribution function

When a concentrated load P acts on a free end of a cantilever beam (Fig. 6), the normal stress can be computed by the 2nd order stress distribution function as formulated by Chang and Zheng (1987).

$$\sigma(x) = \frac{P}{Z}\left[x - \frac{5n}{4K}\left(1 - \frac{y^2}{b'^2} - \frac{2}{3}\frac{I_s}{I}\right)\frac{\sinh Kx}{\cosh KL}\right] \tag{6a}$$

where Z = sectional modulus, $I_s/I = 3/S + 3$, n and K are defined by Eq. (6b) which are based on Reissner's parameters (Reissner 1946), respectively.

$$n = \frac{6S + 18}{6S + 3}, \qquad K = \frac{1}{b'}\sqrt{\frac{14}{10(1 + \nu)}}\sqrt{\frac{6S + 18}{6S + 3}} \tag{6b}$$

Based on Eq. (6a) by Chang and Zheng, a practical formula for b_e/b is derived in this study. When $x=L$ and $L/b' \geq 2.5$, Eq. (6c) can be obtained from Eq. (6a) and Eq. (6b) with $\frac{\sinh Kx}{\cosh KL} \cong 1.0$.

$$\sigma(L) = \frac{P}{Z}\left[L - \frac{5n}{4K} + \frac{5n}{4K}\frac{y^2}{b'^2} + \frac{2}{3}\frac{I_s}{I}\frac{5n}{4K}\right] \tag{6c}$$

If $y = \pm b'$ is substituted into Eq. (6c), the maximum normal stress $\sigma_{\max}$ is obtained. Using the concept of the effective width (Moffat and Dowling 1975, BS5400 1982, Tahan *et al*. 1997), the effective width ratio b_e/b is obtained as follows.

$$\frac{b_e}{b} = \frac{\int_0^{b'}\sigma(L)dy}{b' \cdot \sigma_{\max}} = \frac{L - \frac{5}{6}\frac{n}{K} + \frac{5}{6}\frac{n}{K}\frac{I_s}{I}}{L + \frac{5}{6}\frac{n}{K}\frac{I_s}{I}} \tag{7a}$$

Also, if n/K based on the 2nd stress distribution function and I_s/I are substituted into Eq. (7a), the effective width ratio b_e/b is formulated as follows by the width-span length ratio L/b' and the sectional area ratio S.

$$\frac{b_e}{b} = \frac{\frac{L}{b'} - 0.803\sqrt{\frac{6S+18}{6S+3}} + 2.409\sqrt{\frac{6S+18}{6S+3}}\left(\frac{1}{S+3}\right)}{\frac{L}{b'} + 2.409\sqrt{\frac{6S+18}{6S+3}}\left(\frac{1}{S+3}\right)} \quad \text{for} \quad \frac{L}{b'} \geq 2.5 \tag{7b}$$

3.2.2 The 3rd order stress distribution function

If the distribution of normal stress is assumed by the 3rd order stress distribution function, stress distribution $\sigma(x)$ is expressed as follows.

$$\sigma(x) = \frac{P}{Z}\left[x - \frac{7n}{6K}\left(1 - \frac{y^3}{b'^3} - \frac{3}{4}\frac{I_s}{I}\right)\frac{\sinh Kx}{\cosh KL}\right] \tag{8a}$$

where Reissner's two parameters n and K can be expressed by Eq. (8b) in terms of the sectional area ratio S.

$$n = \frac{8S+24}{8S+3}, \quad K = \frac{1}{b'}\sqrt{\frac{14}{10(1+\nu)}}\sqrt{\frac{8S+24}{8S+3}} \tag{8b}$$

where $\frac{I_s}{I} = \frac{3}{S+3}$.

By following the same procedure as the case of the 2nd order stress distribution function, the effective width ratio of b_e/b for the 3rd order stress distribution function is derived as follows.

$$\frac{b_e}{b} = \frac{\frac{L}{b'} - 0.843\sqrt{\frac{8S+24}{8S+3}} + 2.529\sqrt{\frac{8S+24}{8S+3}}\left(\frac{1}{S+3}\right)}{\frac{L}{b'} + 2.529\sqrt{\frac{8S+24}{8S+3}}\left(\frac{1}{S+3}\right)} \quad \text{for} \quad \frac{L}{b'} \geq 2.5 \tag{9}$$

3.2.3 Higher order stress distribution function

The effective width ratio b_e/b for higher order stress distribution functions can be obtained by the same procedure and are presented in Table 1.

3.3 Comparison of effective width

Fig. 8 compares the effective width ratio b_e/b of a simple beam with that of a cantilever beam using the 2nd order stress distribution function when the span length is L. When the span length of a simple beam and a cantilever is the same as L, the effective width ratios of a cantilever beam are consistently larger than those of a simple beam with equal sectional area ratio. However, when the span length of the simple beam is doubled by $2L$ with fixed span length for the cantilever, the trend of b_e/b from two beam models almost coincide each other at every trial value of L/b' as shown in Fig. 8(b). From the two figures, we can observe that Okumura's approach of calculating shear lag parameter in beam-to-column connections using a simple beam model does not reflect this span length effect properly.

Table 1 The effective width ratio with the different order of stress distribution function

Order of stress distribution function	Effective width ratio (b_e/b)
2	$\dfrac{\frac{L}{b'} - 0.803\sqrt{\frac{6S+18}{6S+3}} + 2.409\sqrt{\frac{6S+18}{6S+3}}\left(\frac{1}{S+3}\right)}{\frac{L}{b'} + 2.409\sqrt{\frac{6S+18}{6S+3}}\left(\frac{1}{S+3}\right)}$
3	$\dfrac{\frac{L}{b'} - 0.843\sqrt{\frac{8S+24}{8S+3}} + 2.529\sqrt{\frac{8S+24}{8S+3}}\left(\frac{1}{S+3}\right)}{\frac{L}{b'} + 2.529\sqrt{\frac{8S+24}{8S+3}}\left(\frac{1}{S+3}\right)}$
4	$\dfrac{\frac{L}{b'} - 0.867\sqrt{\frac{10S+30}{10S+3}} + 2.601\sqrt{\frac{10S+30}{10S+3}}\left(\frac{1}{S+3}\right)}{\frac{L}{b'} + 2.601\sqrt{\frac{10S+30}{10S+3}}\left(\frac{1}{S+3}\right)}$
5	$\dfrac{\frac{L}{b'} - 0.883\sqrt{\frac{12S+36}{12S+3}} + 2.650\sqrt{\frac{12S+36}{12S+3}}\left(\frac{1}{S+3}\right)}{\frac{L}{b'} + 2.650\sqrt{\frac{12S+36}{12S+3}}\left(\frac{1}{S+3}\right)}$

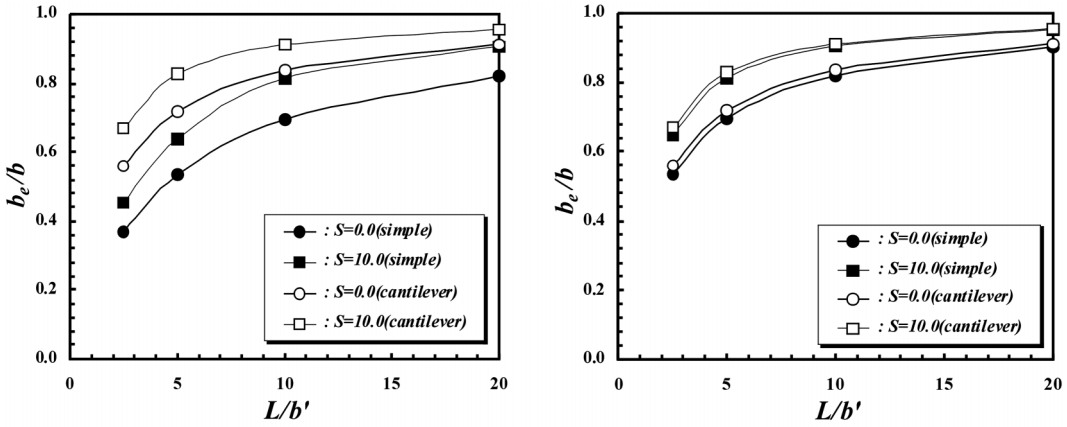

(a) Simple beam span length = L (b) Simple beam span length = $2L$

Fig. 8 Comparison of b_e/b from simple beam and cantilever beam models with variation of L/b'

3.4 Influence of L/b' and S on effective width

The effective width ratio b_e/b of a cantilever beam can be expressed by a function of the width-span length ratio L/b' and the sectional area ratio S as presented in Table 1. Fig. 9(a) shows the

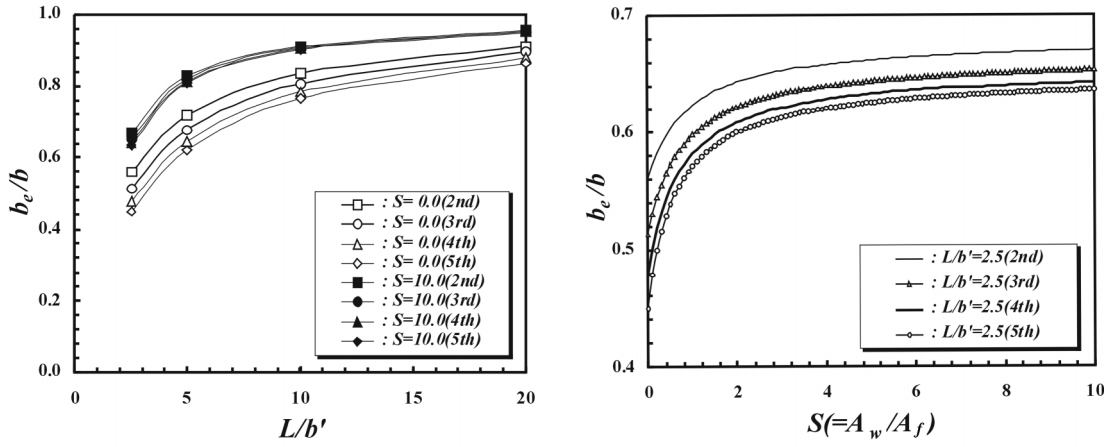

(a) Influence of L/b' on b_e/b (b) Influence of S on b_e/b

Fig. 9 Influence of L/b' and S on effective width ratio

relationships between the effective width ratio and the width-span length ratio depending on the order of stress distribution function when the sectional area ratio S is fixed as either of the value of 0.0 or 10.0. The effective width ratio increases rapidly in the region of small L/b' but gradually converges to a constant value where $L/b' > 10.0$. When the value of $S = 0.0$, the value of the effective width ratio b_e/b increases as the order of stress distribution function decreases. However, when the value of $S = 10.0$, the values of b_e/b do not change with the increase of the order of stress distribution function. Fig. 9(b) shows the variation of the effective width ratio b_e/b with the change of the sectional area ratio S with a fixed value of $L/b' = 2.5$. The effective width ratio increases rapidly in the region of $S < 2.0$ but is not sensitively affected by L/b' when $S > 2.0$. From the observations of Fig. 9, it can be concluded that the influence of L/b' and S should be considered in calculating the effective width ratio b_e/b, especially when $L/b' \leq 10.0$ and $S \leq 2.0$ as usual situation of steel piers.

4. Development of formula for shear lag parameter

4.1 Shear lag parameter η_c considering additional moment

In evaluating shear lag stress due to additional moment, shear lag parameter η_c will be derived based on various stress distribution functions. When a concentrated load P is applied to a cantilever beam with box section as shown in Fig. 7, the additional moment M_f occurs at the flange due to the shear deformation of the web. The additional moment is given by Eq. (10) when the normal stress distribution is assumed as the 2nd order stress distribution function (Chang and Zheng 1987).

$$M_f = \frac{5}{6}\frac{I_s}{I}\frac{n}{K}P \tag{10}$$

where I_s/I, n, K are as defined in Eq. (6). The sectional modulus Z can be expressed by Eq. (11).

$$Z = 2 \cdot A_f \cdot d\left(\frac{3+S}{12}\right) \tag{11}$$

where $A_f = 2b \cdot t_f$.

Then, the shear lag stress σ_s is calculated by dividing the additional moment M_f by the sectional modulus Z as Eq. (12a).

$$\sigma_s = \frac{M_f}{Z} = \frac{5}{6}\frac{I_s}{I}\frac{n}{K}\frac{1}{Z} = 7.227 \times \frac{S}{(3+S)^2}\sqrt{\frac{6S+18}{6S+3}} \cdot \frac{b}{d}\frac{P}{A_w} \tag{12a}$$

By considering concentrated load P as the flange force F_i which acts as shear force at the connection, Eq. (12a) can be rearranged as follows.

$$\sigma_s = \eta_c \cdot \left(\frac{b}{d}\frac{F_i}{A_w}\right) \tag{12b}$$

where η_c = the shear lag parameter considering an additional moment as defined by Eq. (13).

$$\eta_c = 7.277 \times \frac{S}{(S+3)^2}\sqrt{\frac{6S+18}{6S+3}} \tag{13}$$

Similarly, in the case of the 3rd order stress distribution function, the additional moment M_f is given by Eq. (14).

$$M_f = \frac{7}{8}\frac{I_s}{I}\frac{n}{K}P \tag{14}$$

By using a similar procedure as in the 2nd order stress distribution function, the shear lag parameter η_c for the 3rd order stress distribution function can be derived as.

$$\eta_c = 7.589 \times \frac{S}{(S+3)^2}\sqrt{\frac{8S+24}{8S+3}} \tag{15}$$

For a higher order of stress distribution function, the shear lag parameter η_c was derived for the corresponding M_f, n, and K. Table 2 summarizes the formula for shear lag parameter η_c with different orders of stress distribution function.

Table 2 Shear lag parameter with stress distribution function

Order of stress distribution	Shear lag parameter η_c
2	$7.277 \times \frac{S}{(S+3)^2}\sqrt{\frac{6S+18}{6S+3}}$
3	$7.589 \times \frac{S}{(S+3)^2}\sqrt{\frac{8S+24}{8S+3}}$
4	$7.805 \times \frac{S}{(S+3)^2}\sqrt{\frac{10S+30}{10S+3}}$
5	$7.884 \times \frac{S}{(S+3)^2}\sqrt{\frac{12S+36}{12S+3}}$

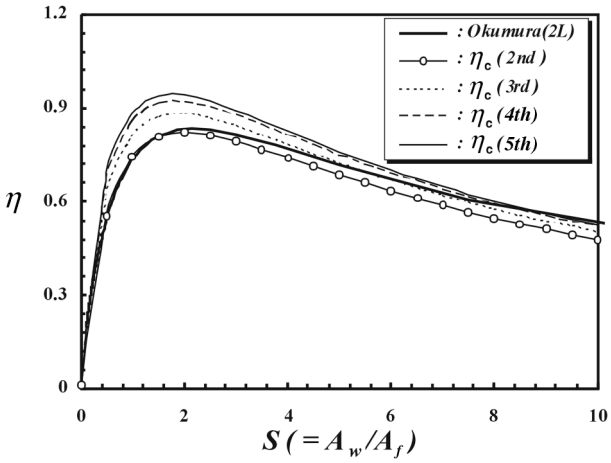

Fig. 10 Variation of shear lag parameter η_c

Fig. 10 shows the relationship between the different shear lag parameter η_c when S varies. The shear lag parameter η_c based on the 2nd order stress distribution function agrees well with the Okumua and Ishizawa's shear lag parameter η_o obtained from a simple beam model if the span length is set equal to $2L$. From the figure, we can also observe that the shear lag parameter η_c becomes larger as the order of stress distribution function increases with a fixed value of S. However, when the order of a stress distribution function is higher than 4, the increase rate of η_c with a fixed value of S reduces rapidly.

4.2 Shear lag parameter η_{eff} based on effective width

As another approach, the shear lag stress can be evaluated by considering the effective width of the flange. If the normal stress of the flange which is increased by using sectional modulus with effective width is assumed as maximum normal stress, the difference between maximum normal stress and average normal stress by elementary beam theory can be defined as shear lag stress σ_s. Then, a shear lag parameter η_{eff} can be derived from shear lag stress σ_s based on effective width.

Z_n and Z is sectional modulus with and without considering the effective width. They are defined as Eq. (16a).

$$Z_n = \frac{A_f d(3 \cdot b_e/b + S)}{6}, \qquad Z = \frac{A_f d(3 + S)}{6} \tag{16a}$$

The difference between the inverse of sectional moduli Z_n and Z is obtained as Eq. (16b).

$$\left(\frac{1}{Z_n} - \frac{1}{Z}\right) = \frac{18(1 - b_e/b)}{A_f d(3b_e/b + S)(3 + S)} \tag{16b}$$

where A_f is the area of the flange plate(= $2bt_f$). Then, the shear lag stress σ_s is obtained by multiplying Eq. (16) by bending moment M as Eq. (17a).

$$\sigma_s = M \cdot \left(\frac{1}{Z_n} - \frac{1}{Z}\right) = \left\{\frac{L}{b}\frac{18(1 - b_e/b)}{(3b_e/b + S)(3 + S)}\right\} \cdot \left(\frac{b}{d}\frac{F_i}{A_w}\right) \tag{17a}$$

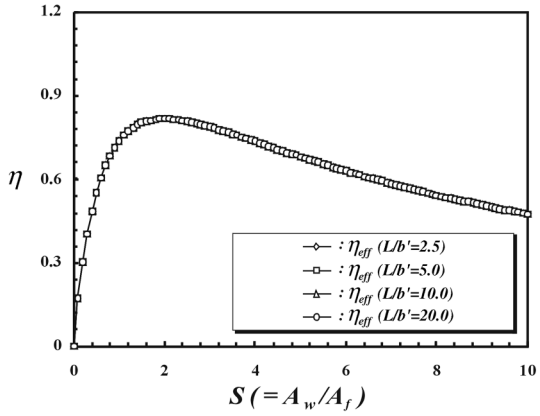

Fig. 11 Variation of η_{eff} with different L/b'

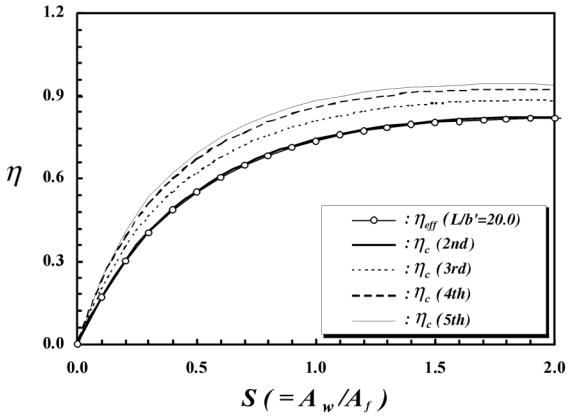

Fig. 12 Comparison of η_c and η_{eff}

Also, by considering concentrated load P as the flange force F_i, Eq. (17a) can be rearranged as follows.

$$\sigma_s = \eta_{eff} \cdot \left(\frac{b}{dA_w} \frac{F_i}{} \right) \tag{17b}$$

where η_{eff} = the shear lag parameter using effective width defined by Eq. (18).

$$\eta_{eff} = \frac{L}{b} \frac{18(1 - b_e/b)S}{(3b_e/b + S)(3 + S)} \tag{17c}$$

Fig. 11 shows the variation of shear lag parameter η_{eff} with respect to the sectional area ratio S with different values of L/b'. From the figure, it is observed that the shear lag parameter η_{eff} of Eq. (18) is not influenced by the change of L/b'. As a result, the shear lag parameter η_{eff} of Eq. (18) can be a function of a single parameter S. Fig. 12 shows a good agreement between the effective shear lag parameter η_{eff} and the shear lag parameter η_c using the 2nd order stress distribution function.

From the two approaches of evaluating shear lag stress in terms of shear lag parameter, both methods by parameter η_c considering additional moment and η_{eff} based on the effective width produce consistent results. Therefore, the shear lag stress may be evaluated by the shear lag parameter η_c which is only dependent on the sectional area ratio S.

5. Comparison with test results

5.1 Test model

The shear lag parameter η_c at a beam-column connection was derived as a function of the sectional area ratio S in Eq. (13), Eq. (15), and Table 2. To verify the theoretical equations for η_c, laboratory experiments have been carried out with a test device shown in Fig. 13(a) and the results in elastic region are compared. The test specimen is hinged at one edge with roller at the other as shown in Fig. 13(b). Four different categories of test specimens (A, B, C, D) were used as

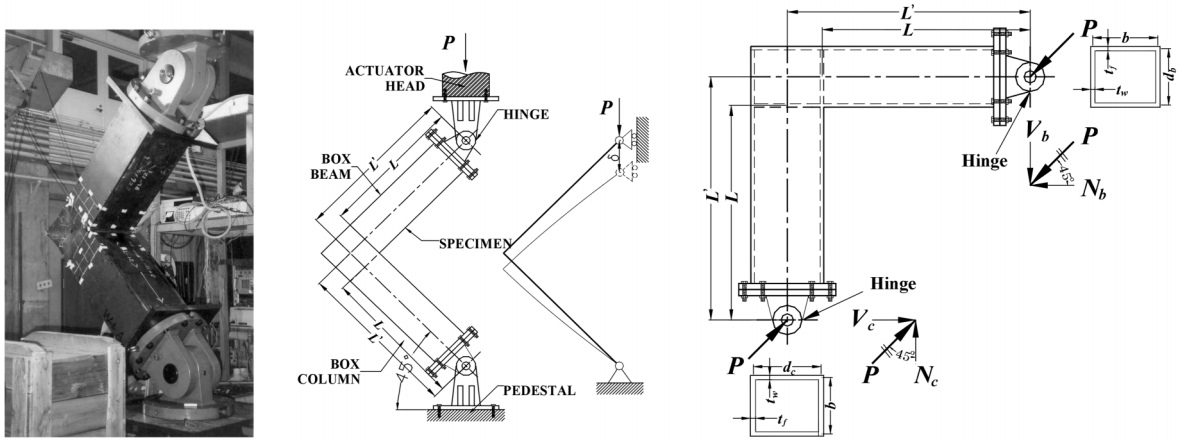

(a) Test device (b) Boundary condition (c) Section details

Fig. 13 Test setup, boundary condition, and section details

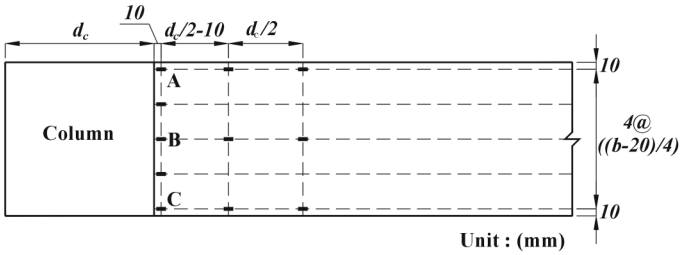

Fig. 14 Gauge locations in the lower flange of beam

summarized in Table 3. Fig. 14 shows the strain gauge layout for the specimens. The maximum normal stresses due to shear lag phenomenon calculated by the data of gauge A and gauge C were used to compare with the analytical solutions. Also, because minimum yield stress of specimens was 286 Mpa, all specimens were in the elastic state under given load *P*. In Table 3, S_{bc} is the sectional area ratio of the beam or column, σ_b is the normal stress by beam theory, $\sigma_{\max}$ is the maximum normal stress from experiments, σ_s is a shear lag stress calculated from $\sigma_{\max} - \sigma_b$, F_i is the concentrated flange force calculated from Eq. (1), and η is the shear lag parameter calculated from experiments based on the form of Eq. (12b), respectively.

5.2 Evaluation of shear lag stress

Fig. 15 compares the shear lag parameters from experimental results (Hwang 1993) with η_c in Table 2 and η_{eff} in Eq. (18). As observed from Fig. 12, the shear lag parameter η_{eff} using the 2nd order stress distribution function and the shear lag parameter η_c from Eq. (18) agree well but these two shear lag parameters are consistently lower than those from the experiments. Also, it can be observed that the upper limit values from the experiments almost coincide with the shear lag parameter by the 5th order stress distribution function. Thus, from the equations in Table 2, the shear lag parameter η_c over the 4th order stress distribution function can be considered to estimate the

Table 3 Shear lag parameters of test model

Model	b (mm)	t_f (mm)	d_b (mm)	d_c (mm)	t_w (mm)	L' (mm)	S_{bc}	P (kN)	σ_b (Mpa)	σ_{max} (Mpa)	σ_s (Mpa)	F_i (kN)	Shear lag parameter η
A-1b*	184.4	5.9	154.1	154.1	4.4	600	0.62	27.7	82.0	156.3	74.3	107924	0.78
A-2b	244.5	6.0	204	204	4.5	800	0.63	42.7	93.6	177.5	83.9	167399	0.77
A-3b	184.5	6.0	204	154	4.5	620	0.83	21.3	45.3	81.5	36.2	64867	0.85
B-1b	275.6	8.8	201.2	201.2	5.6	900	0.46	56.5	91.3	177.8	86.4	252629	0.56
B-2b	335.6	8.8	271.2	271.2	5.6	1100	0.51	56.3	65.9	125.5	59.6	228229	0.64
B-3b	275.6	8.8	271.2	201.2	5.6	900	0.63	58.5	66.1	109.1	42.9	194091	0.66
C-1b	486	11.85	428	428	11.85	2000	0.88	207.9	141.8	215.6	73.8	971436	0.79
C-2b	415	11.85	488	418	11.85	2000	1.18	69.3	41.1	63.7	22.6	324762	0.94
C-3c**	415	11.85	488	418	11.85	2000	1.01	69.3	48.8	75.0	26.1	288117	0.90
D-1b	306	10.0	270	190	6.0	900	0.53	39.2	37.8	73.5	35.7	136474	0.75
D-1c	306	10.0	270	190	6.0	900	0.37	39.2	52.8	112.9	60.1	177432	0.48
D-2b	308	10.0	330	260	8.0	1300	0.86	39.2	39.5	60.8	21.3	158582	0.76
D-2c	308	10.0	330	260	8.0	1300	0.68	39.2	50.8	88.2	37.4	190723	0.69
D-3b	336	8.0	232	172	6.0	900	0.52	39.2	49.8	107.8	58.0	157138	0.71
D-3c	336	8.0	232	172	6.0	900	0.38	39.2	66.8	161.2	94.4	198279	0.50
D-4b	338	8.0	292	232	8.0	1300	0.86	39.2	50.7	88.2	37.5	178548	0.85
D-4c	338	8.0	292	232	8.0	1300	0.69	39.2	64.9	127.4	62.5	214586	0.74

* : b index means experimental data of the beam lower flange
** : c index means experimental data of the column lower flange

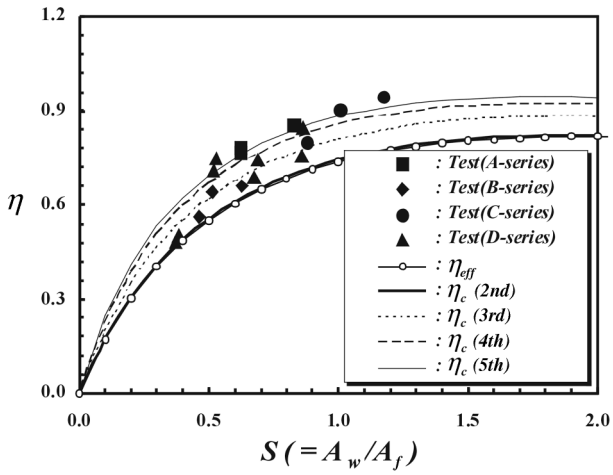

Fig. 15 Comparison of η_c with test results

upper limit value. Therefore, it may be reasonable to use the shear lag parameter η_c by using the 4th order stress distribution function to evaluate the shear lag stress properly.

6. Conclusions

To evaluate the shear lag stress at a beam-to-column connection of steel piers, two types of shear lag parameters, i.e., η_c derived from an additional moment and η_{eff} based on the effective width ratio b_e/b in a cantilever beam have been derived in a different way. From the study, the following conclusions could be obtained:

1) A cantilever beam model was identified as a proper model to evaluate shear lag stress at beam-to-column connection rather than a simple beam model. In this study, therefore, equations for effective width of cantilever beam with hollow rectangular section were derived using a cantilever model based on the 2nd through 5th order stress distribution functions.
2) The effective width ratio b_e/b of a cantilever calculated from derived equation changes rapidly when the width-span length ratio $L/b' < 10.0$ and the sectional area ratio $S < 2.0$.
3) The shear lag parameter η_{eff} based on the effective width is in a good agreement with η_c obtained by using the 2nd order stress distribution function. Therefore, the shear lag stress can be evaluated by the shear lag parameter η_c which is only dependent on the sectional area ratio S.
4) Because the shear lag parameter η_c using a stress distribution function with a higher than the 4th order almost converges to the upper bound of shear lag parameters from the experiments, it seems to be reasonable to apply the shear lag parameter η_c with the 4th order stress distribution function for evaluating shear lag stress σ_s.

Although the shear lag stress can be properly evaluated from the proposed parameter η_c for a typical rectangular beam-to-column connection, considerations on the variable section and yielding pattern of connections may be also necessary to develop design equations of steel pier connection in near future.

References

Beedle, L.S., Topractsoglou, A.A. and Jonhston, B.G. (1951), "Connection for welded continuous portal frames", *Welding Journal*, **30**, 354s-384s.

BS5400 (1982), "Steel concrete and composite bridges, Parts 3 and 5 : Code of practice for design of composite bridges", British Stand Institution, London.

Chang, S.T. and Zheng, F.Z. (1987), "Negative shear lag in cantilever box girder with constant depth", *J. Struct. Engrg.*, ASCE, **113**(1), 20-35.

Fafitis, A. and Rong, A.Y. (1995), "Analysis of thin-walled box girders by parallel processing", *Thin-walled Struct.*, **21**, 233-240.

Fielding, D.J. and Huang, J.S. (1971), "Shear in steel beam-to-column connections", *Welding Journal*, **50**(7), 313s-326s.

Hwang, W.S. (1993), "Inelastic behavior and provisions for limit state design of beam-to-column connections in steel bridge pier structures", PH. D. thesis, Osaka University of Japan.

Komatsu, S. (1974), *Theory and Design of Thin-Walled Structures*, SanKaiDou(in Japanese).

Kuzmanović, B.O. and Graham, H.J. (1981), "Shear lag in box girder", *J. Struct. Div.*, ASCE, **107**(9), 1701-1742.

Lee, C.K. and Wu, G.J. (2000), "Shear lag analysis by the adaptive finite element method-1. Analysis of simple plated structures", *Thin-walled Struct.*, **38**, 285-309.

Luo, Q.Z., Tang, J. and Li, Q.S. (2002), "Experimental studies on shear lag of box girder", *Eng. Struct.*, **24**, 464-477.

Malcolm, D.J. and Redwood, R.G. (1970), "Shear lag in stiffened box girders", *J. Struct. Div.*, ASCE, **96**(ST7), 1403-1449.

Moffat, K.R. and Dowling, P.J. (1975), "Shear lag in box girder bridges", *Struct. Engrg*., **53**, 439-448.
Nakai, H., Miki, T. and Hashimoto, Y. (1992), "On limit state design method considering shear lag phenomenon of corner parts of steel rigid frames", *JSCE*, **455**, 95-104(in Japanese).
Okumura, T. and Ishizawa, N. (1968), "The design of knee joints for rigid steel frames with thin walled section", *JSCE*, **153**, 1-17(in Japanese).
Reissner, E. (1946), "Analysis of shear lag in box beams by the principle minimum potential energy", *Quarterly App. Math*., **3**(3), 268-278.
Tahan, N., Palović, M.N. and Kotsovos, M.D. (1997), "Shear-lag revisited : The use of single Fourier series for determining the effective breadth in plated structures", *Computers & Structures*, **63**(4), 759-767.
Tesar, A. (1996), "Shear lag in the behavior of thin walled box bridge", *Computers & Structures*, **59**(4), 607-612.
Timoshenko, S.P. and Goodier, J.N. (1987), *Theory of Elasticity*, 3rd ed., McGraw-Hill, 267-268.
Wang, Q.F. (1997), "Lateral buckling of thin-walled members with openings considering shear lag", *Structural Engineering and Mechanics*, **5**(4), 369-383.